Journal of Hydraulic Structures
J. Hydraul. Struct., 2025; 11(1): 41-50
DOI: 10.22055/jhs.2024.47215.1304

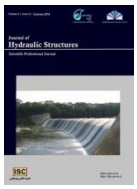

OPEN ACCESS

Spiral Flow Measurement at Vertical Intakes Using PTV Method

ShahWali Hamidi[1]
Hamed Sarkardeh[1*]
Ali Bashtani[1]

Abstract

In order to study the characteristics of the different formed free surface vortices at vertical hydraulic intakes, three sets of experiments were conducted. The spiral flow was detected using the Particle Tracking Velocimetry (PTV) measurement technique in three dimensions (3D) by installing two cameras at above and side of the model. The dimensions of model were 2000mm in length, 1300mm in width and 1500mm in height. Through the experiments, extensive data including tangential (V_θ), radial (V_r) and axial (V_z) velocities and their variations with the changing vortex center in different vortex classes, were recorded and analyzed. Using the obtained results, a 3D flow path was drawn for each class of the formed vortex. Moreover, changes in the diameter of the vortex core (D_{vo}) in the three different classes of vortex were investigated and its changes along the vortex axis were measured. Results showed that the average of D_{vo}/D (D is the intake diameter) was about 0.14, 0.2 and 0.23 for vortices Class C, B and A, respectively.

Keywords: Spiral Flow; Free Surface Vortex; Vertical Intake; PTV Method; Vortex core diameter.

Received: 24 June 2024; Accepted: 10 September 2024

Notations

D: intake diameter
Fr: intake Froude number = $V/(gD)^{1/2}$
g: gravitational acceleration
Q: intake discharge
Re: intake Reynolds number = VD/υ
r: radial distance from the vortex center
S: submergence of the intake centerline
S/D: relative submergence of the intake

*Email: sarkardeh@hsu.ac.ir
[1]Department of Civil Engineering, Hakim Sabzevari University, Sabzevar, Iran.

We: intake Weber number = $\rho V^2 D/\sigma$
ρ: density of water
σ: surface tension of water
v: kinematic viscosity of water
V_θ: tangential velocity component
V_r: radial velocity component
V_z: axial velocity component
Z/s: relative depth
D_{vo}: diameter of the vortex core

1. Introduction

The occurrence of free surface vortex in reservoirs is a common and damaging event, posing a significant challenge in hydraulic engineering for intake design. The impact of these vortices can lead to severe damage to the hydraulic structures, especially hydraulic machinery, due to sudden pressure changes and shocks. This can result in inducing vibrations, noise pollution, decreasing the operational efficiency of hydraulic equipment, and moving debris and sediments into the intake. Forming air-core vortices can disrupt the expected forces on turbine blades, reducing power plant performance and increasing hydraulic losses during power generation [1-3]. Sarkardeh et al. categorized free surface vortices into three classes based on their strength and associated risks [4]. Class C represents weak and safe rotations, while Class B involves flow rotation reaching the intake and dragging debris. Class A denotes the strongest vortices that should be avoided, where air bubbles are trapped and drawn down to the intake. In the most intense state, a stable air-core forms at the vortex center, steadily drawing air into the intake (Figure 1).

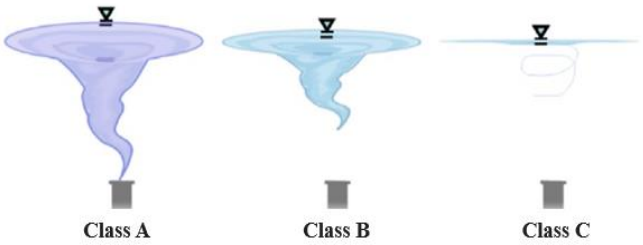

Figure 1. Classification of vortices based on their strength [4]

Some performed researches in the recent years, making significant contributions to the progress of knowledge in the field of hydraulic engineering. Sarkardeh and Marosi analytically recognized and analyzed the spiral flow motion of the free surface vortices at intakes [5]. Azarpira and Zarrati [6] created a precise computational model designed for the analysis of 3D air-core vortices. Suerich-Gulick et al. introduced a model for predicting the fundamental attributes of free surface vortices at intake [7,8]. Wang et al. [9] have conducted various studies on the evolution of vortices. Recently, numerical simulations have a significant effect on exploring different characteristics and aspects of free surface vortices at intakes [10-17]. Pakdel et al. conducted a numerical study to examine the impact of waves on vortices that are generated in vertical intakes [18-19]. Zi et al. [20] investigated formation and development mechanism of the air-core vortex situated between the free surface and the horizontal flow intake. Many aspects of vortex formation were discovered through the use of physical models [21-27]. Monshizadeh et al. and Tahershamsi et al. conducted a comparative study and analysis on

dynamic of a formed free surface vortex at horizontal intakes and also a hydraulic method on dissipating formed vortices [28-32]. Aghajani et al. investigated the effect of a trash rack at the entrance of intake on strength of formed vortices using an experimental model [33,34]. Amiri et al. investigated methods for preventing vortices by various anti-vortex plates [35]. Camnasio et al. conducted an experimental investigation on the velocity distributions within rectangular shallow reservoirs using ultrasound profiling. They aimed to assess how the reservoir geometry influences the flow patterns [36]. In an experimental study, Sarkardeh et al. [37] investigated the 3D components of velocity using an Acoustic Doppler Velocimetry (ADV) device in a reservoir with a horizontal intake. Suerich-Gulick et al. [8] have utilized Particle Image Velocimetry (PIV) to analyze the vortex flow field.

Although a large number of studies were conducted in the field of vortex recognition to date, there are still many problems to be solved due to the complexity of the vortex. The purpose of this study is to utilize the PTV technique to visualize the spiral flow and determine the 3D velocity components in different free surface vortices. In the present research, by employing a big experimental model, V_θ, V_r and V_z were determined using the PTV technique. Regarding the measured different velocity components, 3D spiral flow path line was drawn for three different classes of vortices. Moreover, diameter variations of the vortex core in each class were also recorded and analyzed.

2. Methods and Materials

2.1. Experimental setup

The used physical model consisted of a metal structure with 10mm thickness glass walls to provide a clear view of the reservoir sides and bottom [38]. The reservoir had dimensions of 2000mm in length, 1300mm in width, and 1500mm in height, with water capacity of approximately 4m³ . To minimize the scale effects, Reynolds (*Re*) and Weber (*We*) should be greater than a value which suggested by the different researchers to neglect the effects of viscosity and surface tension. Considering the effects of viscosity and surface tension in vortex modeling and creating scale errors, by summarizing the opinions of different researchers and maintaining the appropriate margin of safety in model design, *Re* and *We* should have a value greater than $Re \geq 1.1 \times 10^5$ and $We \geq 720$ [38]. The reservoir length was 2000mm to ensure undisturbed flow to the test area after passing through flow energy dissipaters (Figure 2).

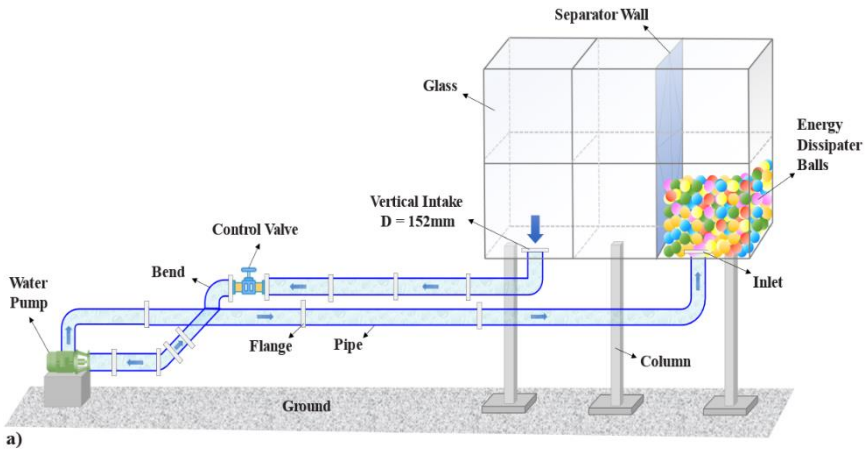

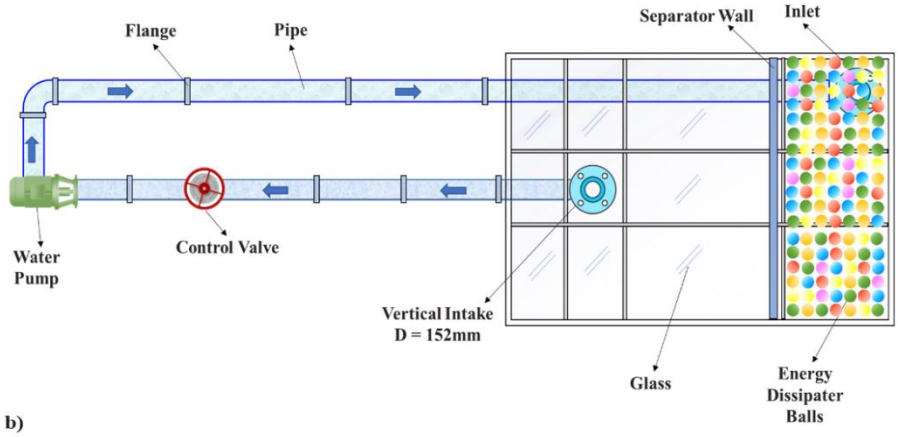

Figure 2. Side Schematic view (a), top schematic view (b)

2.2. Measurement technique

To prevent interruption in the flow, the PTV method was utilized to measure the 3D velocity distributions and plot the spiral flow path lines. In this system, a pair of 5-megapixel cameras was utilized, capable of recording videos at a frame rate of 25 fps. The importance of using these types of cameras was ability of synchronizing when recording starts and ends. In this investigation, because of low speed of motion, the tracer particles can be easily identified without the need for high image resolution and also high frame rate of camera. By installing an up view camera on the base of the tank, images related to the x-y coordinate plane can be recorded. By utilizing the camera positioned on the ground base, side-view images can be captured in the x-z coordinate plane. Two cameras can simultaneously send the recorded images to the Digital Video Recorder (DVR) device for storage. The images recorded on the DVR can be reviewed on the monitor and exported as video files for further processing (Figure 3).

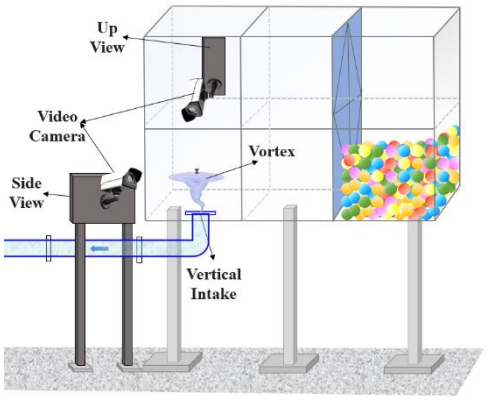

Figure 3. Imaging equipment

2.3. Experimental procedure

In this research, three classes of vortices are formed by adjusting the flow rate of the pump connected to the reservoir. Three different flow rates result in the generation of vortices in three

classes of C, B, and A, at a constant relative submerged depth (*S*/*D*). In order to create a stable vortex at the entrance of the vertical intake, each test required a minimum time of 15 minutes to establish stable conditions. After establishing stable conditions in each vortex class, a tracer particle was released into the test area in the reservoir, and its movement is recorded in the x-y and x-z coordinates. The recorded videos were divided into the frames. In this case, the spiral flow path line is drawn for each vortex class, and the 3D velocity parameters were determined based on the center of the formed vortex. The PTV method consists of several key steps. First, the tracer particle images acquired in each recording must be analyzed by removing any disturbing backgrounds. After that, the position of each particle must be determined with high accuracy at any time. The subsequent stage entails associating particle images that related to the same physical tracer, usually by identifying the image pair with the shortest distance as the accurate match. In the next step, by grouping the specified points into specific time intervals, it is possible to draw the spiral flow lines and determine the 3D velocity parameters. The PTV method offers several advantages. First, the velocity data obtained is relatively accurate because each velocity vector corresponds to the image of a particle. This characteristic guarantees that measurements remain unaffected by bias errors resulting from spatial averaging [39].

3. Results and Discussions

3.1. Vortex appearance at the intake entrance

The physical model used in this study was capable of simulating all three classes of vortices in terms of strength (Figure 4). Therefore, the physical model was capable to generate flows with varying *Fr* for a constant depth of water in the reservoir. By increasing the flow rate of the pump in the physical model, *Fr* was increased in a constant reservoir water level, leading to the change of the vortex from Class C to Classes B and A. Increasing *Fr* results in the formation of stronger vortices in the laboratory model [4].

Class A **Class B** **Class C**

Figure 4. Vortex formed in the physical model [38]

By forming vortices in three different classes (A, B and C), tracer particles (polystyrene tracer particles with a density similar to the water) were released into the intake area. Using image recording equipment, the trajectory of the tracer particle is visualized in two directions: up and side views of flow (Figure 5).

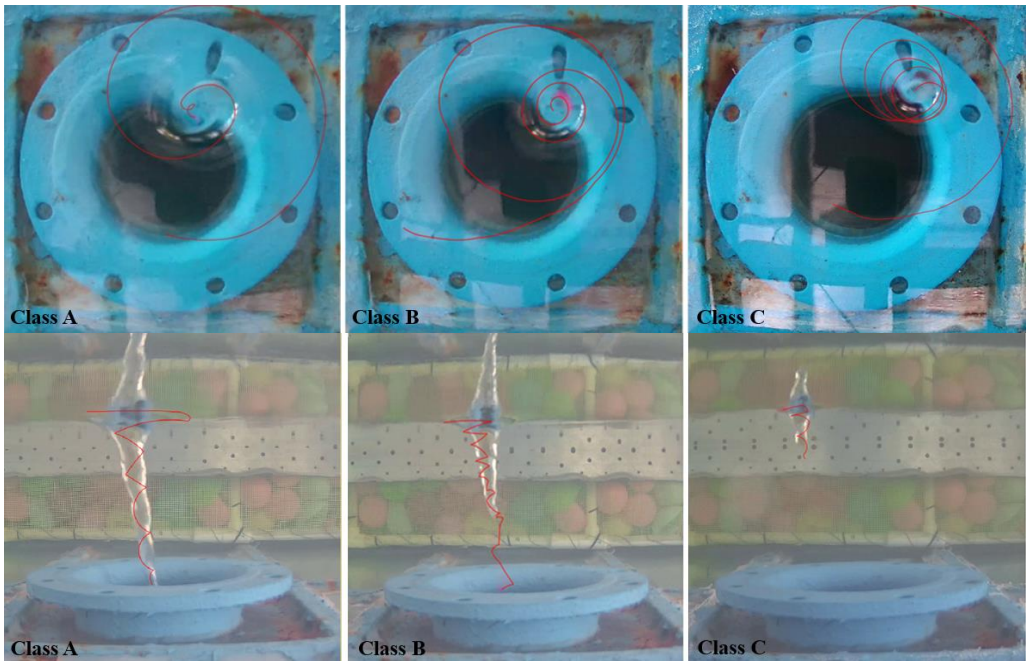

Figure 5. Tracer particle path in up and side views

3.2. Vortex core diameter variations

Figure 6 illustrates the variations in the funnel shape of the vortex across different classes, as well as the changes in the diameter of the vortex core.

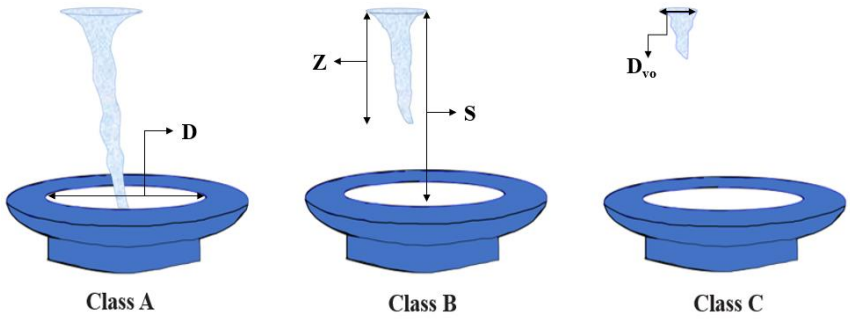

Figure 6. Schematic image of vortex core diameter in three vortex classes A, B and C

Based on the changes in the diameter of the vortex core along the vortex axis (Z) in relation to the intake submergence (s) and considering the Z/s criterion, the variations in the vortex core diameter were examined. The changes of D_{vo} in relation to D were also investigated. Results of D_{vo} changes along the three different formed classes of vortex indicate that Class A has the largest D_{vo} while Class C has the smallest D_{vo}. It is evidence that the maximum of D_{vo} occurs at Z/s = 1 and towards the intake decreases (Figure 7).

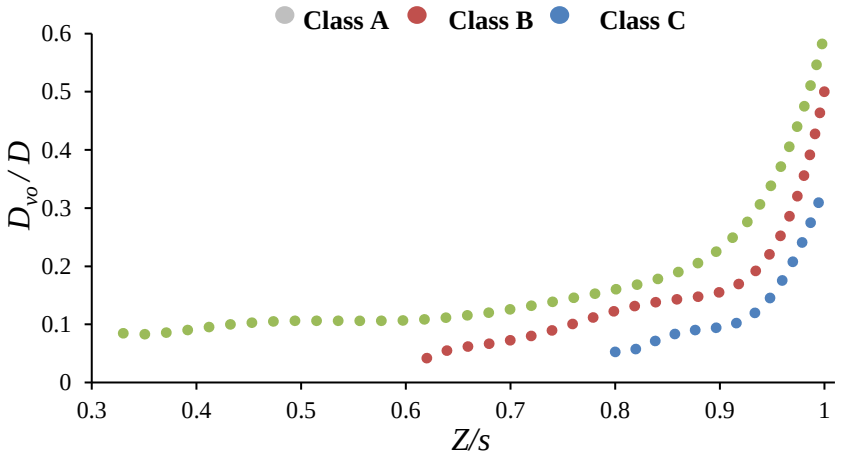

Figure 7. Changes in D_{vo} along the vortex axis at three different classes

The average of D_{vo}/D is about 0.14, 0.2 and 0.23 for vortices Class C, B and A, respectively. This trend demonstrates the impact of increasing the strength of the vortex on the diameter of the vortex core.

3.3. Drawing the spiral path lines

By drawing the flow paths regarding side and top views, three classes of vortex were determined. The output images from top view camera shows a surface spiral path. In Class A vortices, characterized by high flow rate and velocities higher than those of Classes B and C vortices, particles follow a shorter path. This causes their radius of movement to be decreased, rapidly, towards the center of the vortex. The difference in path lengths between Class C and B vortices can be attributed to the tracer particle position within the formed core in the Class C vortex, resulting in rotational movement. In Class A vortex, where there is a higher speed and flow rate than the other two classes of vortex, the tracer particle travels about 30% less distance than the tracer particles in Classes B and C vortices (Figure 8).

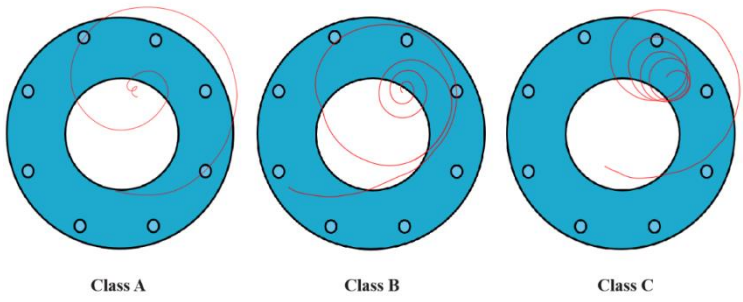

Figure 8. The path line of the tracer particle in an up view

Upon entering the radial range of the vortex, the tracer particles are attracted towards the center of the vortex and become visible in the output images captured by the vision camera positioned at the well side of the funnel-shaped path. In a Class A vortex, a stable air core is formed in the center of the vortex, trapping and transporting air bubbles from the water surface to the intake. Due to the presence of a strong air core in the center of the vortex, the tracer

particle travels a path that is 15% longer than the movement of the tracer particle in the Class B vortex. Figure 9 illustrates the rapid movement of the particle towards the intake in different vortex classes. The path traveled by the tracer particle in Classes A and B vortices is approximately twice as long as the path of the tracer particle in the Class C vortex (Figure 9).

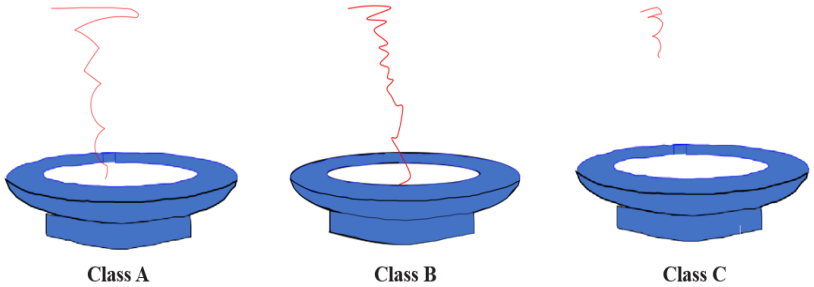

Figure 9. The path line of the tracer particle in a side view

4. Summary and Conclusions

In this study, a rectangular vortex tank with dimensions of 2000 mm in length, 1500 mm in height, and 1300 mm in width was utilized to examine the characteristics of the free surface vortex. The PTV method was used to measure the vortex flow field. In this study, the changes of D_{vo} and the flow path in different classes of vortices have been investigated. In this research, the impact of different vortex classes on flow paths was investigated using the PTV method. The tracer particle in a Class A vortex travels about 30% shorter than in Classes B and C vortex. Also, the tracer particle in the Class B vortex, which experiences more significant changes in radius compared to the Class C vortex, follows a path approximately same and eventually enters the center of the vortex. The tracer particle in Class C travels also same the particle path in the Class B vortex. Although the difference in path length is small, this path occurs over a longer period of time compared to the Class B vortex due to the lower flow velocity to the intake and the weaker strength of the vortex.

Conflict of Interest: The authors declare that they have no conflict of interest.
Availability of Data: The data that supports the findings of this study are available within the article.

References

1. Lugt HJ (1983). Vortex Flow in Nature and Technology. J. Wiley.
2. Knauss J (1987). Swirling flow problems at intakes. Hydraulic Struc. Design Manual. Balkema.
3. Jorabloo M, Abdolahpour M, Roshan R, Sarkardeh H (2011). A techno-economical view on energy losses at hydropower dams (case study of Karun III Dam and Hydropower Plant). Computational Methods in Multiphase Flow VI. 70, 253.
4. Sarkardeh H, Zarrati AR, Roshan R (2010). Effect of intake head wall and trash rack on vortices, J. Hydraulic Research, 48(1): 108–112.
5. Sarkardeh H, Marosi M (2022). An analytical model for vortex at vertical intakes. *Water Supply* 22(1): 31-43.

6. Azarpira M, Zarrati AR (2019) A 3D analytical model for vortex velocity field based on spiral streamline pattern. Water Sci Eng 12:244–252.
7. Suerich-Gulick F, Gaskin SJ, Villeneuve M, Parkinson E (2014). Characteristics of free surface vortices at low-head hydropower intakes. J Hydraul Eng 140(3):291–299.
8. Suerich-Gulick F, Gaskin S, Villeneuve M, Parkinson É (2014c). Free surface intake vortices: Theoretical model and measurements. J. Hydraul. Res., 52(4), 502–512.
9. Wang Y, Jiang C, Liang D (2011a). Comparison between empirical formulae of intake vortices. Journal of Hydraulic Research, 49(1), 113–116.
10. Sarkardeh H, Zarrati AR, Jabbari E, Marosi M (2014). Numerical simulation and analysis of flow in a reservoir in the presence of vortex. Engineering Applications of Computational Fluid Mechanics. 8(4): 598-608.
11. Khadem Rabe B, Ghoreishi Najafabadi SH, Sarkardeh H (2017). Numerical simulation of air-core vortex at intake. CURRENT SCIENCE. 113(1): 141-147.
12. Sarkardeh H (2017). Numerical calculation of air entrainment rates due to intake vortices. Meccanica. 52: 3629-3643.
13. Khadem Rabe B, Ghoreishi Najafabadi SH, Sarkardeh H (2018). Numerical simulation of anti-vortex devices at water intakes. Proc. Inst. Civ. Eng. Water Manag. 171(18).
14. Esmaeilpoor E, Sarkardeh H, Jabbari E (2021). Numerical Study on Simultaneous Operation of Spillway and Power Intake. Journal of Dam and Hydroelectric Powerplant. 8(30), 33-42 (in Persian).
15. Taghizadeh AH, Sarkardeh H, Jabbari E (2023). Numerical study on effect of reservoir vortex on velocity distribution profile in pipe. The European Physical Journal Plus. 138(6), 521.
16. Mousavinia SH, Sarkardeh H, Jabbari E, Taghizadeh AH (2024). Performance of plate and perforated trashracks on vortex prevention at vertical intake. Meccanica. 59(4): 539-559.
17. Amini AA, Sarkardeh H, Jabbari E, Eidi A (2024). Understanding vortex characteristics in hydraulic systems: a temperature-driven analysis. Modeling Earth Systems and Environment, 1-13.
18. Pakdel E, Majdzadeh Tabatabai MR, Sarkardeh H, Ghoreishi Najafabadi SH (2020). Elimination of vortices by wave generation as a hydraulic anti-vortex method. J Braz Soc Mech Sci Eng 42(11):1–14.
19. Pakdel E, Sarkardeh H, Ghoreishi Najafabadi SH (2019). Numerical simulation of the effect of waves on the vortex formed in the vertical intake. Modares Civil Eng J. 19(5):59–71 (in Persian).
20. Zi D, Xuan A, Wang F, Shen L (2020). Numerical study of mechanisms of air-core vortex evolution in an intake flow. Int J Heat Fluid Flow 81:108517.
21. Khodashenas SR, Roshan R, Sarkardeh H, Azamatullah H (2010). Vortex study at orifice spillways of Karun 3 Dam, J. Dam Eng. 11:131–143.
22. Taghvaei SM, Roshan R, Safavi K, Sarkardeh H (2012). Anti-vortex structures at hydropower dams. Int J Phys Sci 7(28):5069–5077.
23. Azarpira M, Sarkardeh H, Tavakkol S, Roshan R, Bakhshi H (2014). Vortices in dam reservoir: a case study of Karun III dam. Sadhana 39(5):1201–1209.
24. Khanarmuei MR, Rahimzadeh H, Sarkardeh H (2015). Investigating the effect of intake withdrawal direction on critical submergence and strength of vortices. Modares Mechanical Engineering 14 (10), 35-42 (in Persian).
25. Khanarmuei MR, Rahimzadeh H, Kakuei AR, Sarkardeh H (2016). Effect of vortex formation on sediment transport at dual pipe intakes. Sadhana 41(9):1055–1061.

26. Sarkardeh H (2017). Minimum reservoir water level in hydropower dams. Chin J Mech Eng 30(4):1017–1024.
27. Khanarmuei MR, Rahimzadeh H, Sarkardeh H (2019). Effect of dual intake direction on critical submergence and vortex strength, Journal of Hydraulic Research, 57 (2), 272-279.
28. Monshizadeh M, Tahershamsi A, Rahimzadeh H, Sarkardeh H (2017). Experimental investigation of dynamics of the air-core vortices and estimating the air entrainment rate at a horizontal intake. Modares Mechanical Engineering. 17 (8), 59-67 (in Persian).
29. Monshizadeh M, Tahershamsi A, Rahimzadeh H, Sarkardeh H (2017). Comparison between hydraulic and structural based anti-vortex methods at intakes. The European Physical Journal Plus 132, 1-11.
30. Monshizadeh M, Tahershamsi A, Rahimzadeh H, Sarkardeh H (2018). Vortex dissipation using a hydraulic-based antivortex device at intakes. International Journal of Civil Engineering 16, 1137-1144.
31. Tahershamsi A, Rahimzadeh H, Monshizadeh M, Sarkardeh H (2018). A new approach on anti-vortex devices at water intakes including a submerged water jet. The European Physical Journal Plus, 133(4):143.
32. Tahershamsi A, Monshizadeh M, Rahimzadeh H, Sarkardeh H (2018). An experimental study on free surface vortex dynamics. Meccanica, 1-9.
33. Aghajani N, Karami H, Mousavi SF, Sarkardeh H (2019). Experimental study of the effect of the trashrack on the vortex at the intake of the hydroelectric power plants in various flow rates and submergence depths. Journal of Dam and Hydroelectric Powerplant, 6(21):49-62 (in Persian).
34. Aghajani N, Karami H, Sarkardeh H, Mousavi SF (2020). Experimental and numerical investigation on effect of trash rack on flow properties at power intakes. ZAMM-Journal of Applied Mathematics and Mechanics, 100(9).
35. Amiri SM, Zarrati AR, Roshan R, Sarkardeh H (2011). Surface vortex prevention at power intakes by horizontal plates. Proceedings of the Institution of Civil Engineers – Water Management 164(4): 193–200.
36. Camnasio E, Orsi E, Schleiss AJ (2011). Experimental study of velocity fields in rectangular shallow reservoirs. Journal of Hydraulic Research, 49(3), 352-358.
37. Sarkardeh H, Jabbari E, Zarrati AR, Tavakkol S (2014). Velocity field in a reservoir in the presence of an air-core vortex. Proc Inst Civ Eng Water Manag 167(6):356–364.
38. Bashtani A, Sarkardeh H (2022). Design of an Experimental Setup for Free Surface Vortex at Intakes (Including a Review on the Constructed Laboratory Models). *Journal of Hydraulic Structures*, *8*(2), 68-83.
39. Raffel M, Willert CE, Scarano F, Kähler CJ, Wereley ST, Kompenhans J (2018). Particle image velocimetry: a practical guide. springer.